

## Study of valence-band intersublevel transitions in InAs/GaAs quantum dots-in-well infrared photodetectors

Yan-Feng Lao, Seyoum Wolde, A. G. Unil Perera, Y. H. Zhang, T. M. Wang, J. O. Kim, Ted Schuler-Sandy, Zhao-Bing Tian, and S. S. Krishna

Citation: [Applied Physics Letters](#) **104**, 171113 (2014); doi: 10.1063/1.4875239

View online: <http://dx.doi.org/10.1063/1.4875239>

View Table of Contents: <http://scitation.aip.org/content/aip/journal/apl/104/17?ver=pdfcov>

Published by the [AIP Publishing](#)

---

### Articles you may be interested in

[An intermediate-band-assisted avalanche multiplication in InAs/InGaAs quantum dots-in-well infrared photodetector](#)

Appl. Phys. Lett. **98**, 073504 (2011); 10.1063/1.3554758

[Temperature-dependent carrier tunneling for self-assembled InAs/GaAs quantum dots with a GaAsN quantum well injector](#)

Appl. Phys. Lett. **96**, 151104 (2010); 10.1063/1.3396187

[Two photon absorption in quantum dot-in-a-well infrared photodetectors](#)

Appl. Phys. Lett. **92**, 023501 (2008); 10.1063/1.2833691

[Origin of photocurrent in lateral quantum dots-in-a-well infrared photodetectors](#)

Appl. Phys. Lett. **88**, 213510 (2006); 10.1063/1.2207493

[Intersublevel transitions in InAs/GaAs quantum dots infrared photodetectors](#)

Appl. Phys. Lett. **73**, 2003 (1998); 10.1063/1.122349

---



Free online magazine

# MULTIPHYSICS SIMULATION

[READ NOW ▶](#)

The COMSOL logo consists of a small red square followed by the word 'COMSOL' in a bold, sans-serif font.

## Study of valence-band intersublevel transitions in InAs/GaAs quantum dots-in-well infrared photodetectors

Yan-Feng Lao,<sup>1</sup> Seyoum Wolde,<sup>1</sup> A. G. Unil Perera,<sup>1,a)</sup> Y. H. Zhang,<sup>2</sup> T. M. Wang,<sup>2</sup> J. O. Kim,<sup>3</sup> Ted Schuler-Sandy,<sup>3</sup> Zhao-Bing Tian,<sup>3</sup> and S. S. Krishna<sup>3</sup>

<sup>1</sup>Department of Physics and Astronomy, Georgia State University, Atlanta, Georgia 30303, USA

<sup>2</sup>Key Laboratory of Artificial Structures and Quantum Control, Department of Physics and Astronomy, Shanghai Jiao Tong University, Shanghai 200240, China

<sup>3</sup>Center for High Technology Materials, Department of Electrical and Computer Engineering, University of New Mexico, Albuquerque, New Mexico 87106, USA

(Received 21 February 2014; accepted 24 April 2014; published online 2 May 2014)

The *n*-type quantum dot (QD) and dots-in-well (DWELL) infrared photodetectors, in general, display bias-dependent multiple-band response as a result of optical transitions between different quantum levels. Here, we present a unique characteristic of the *p*-type hole response, a well-preserved spectral profile, due to the much reduced tunneling probability of holes compared to electrons. This feature remains in a DWELL detector, with the dominant transition contributing to the response occurring between the QD ground state and the quantum-well states. The bias-independent response will benefit applications where single-color detection is desired and also allows achieving optimum performance by optimizing the bias. © 2014 AIP Publishing LLC. [<http://dx.doi.org/10.1063/1.4875239>]

A recent report of *p*-type quantum dot infrared photodetector (QDIP) has shown promising results for using hole transitions to develop photodetectors, with the external quantum efficiency (QE) of 17% being demonstrated.<sup>1</sup> Widely studied *n*-type QDIPs and dots-in-well (DWELL) detectors are featured with the characteristics of multicolor and bias selectivity.<sup>2,3</sup> The optimized bound-to-bound transitions in a GaAs-based *n*-type DWELL structure have led to the achievement of 12% QE.<sup>4</sup> A basic question regarding the *p*-type hole response is to confirm the similar features of multicolor and bias selectivity or to understand the operating mechanism in *p*-type QDIPs and DWELL detectors. Understanding this is of paramount importance to applications, for example, in order to design desired wavelength of detection by employing the DWELL architecture<sup>2</sup> as well as developing QD-based optoelectronic devices.<sup>5</sup> In contrast to a variety of reports on *n*-type electron response, only limited studies using *p*-type optical transitions have been reported.<sup>6–8</sup>

Major differences of the hole states from the electron counterparts originate from the heavier effective mass of holes and three sets of QD states, associated with three branches of the valence bands, i.e., the heavy-hole (HH), light-hole (LH), and spin-orbit split-off (SO) bands. This essentially results in much denser hole levels compared to electrons<sup>1</sup> and the possibility of many optical transitions between them. One may expect a spectral response consisting of multiple bands, each of which becomes active under bias.<sup>3</sup> However, in a recent demonstration of the *p*-type InAs/GaAs QDIP,<sup>1</sup> the dominant response is due to one of the transitions throughout the electric field ranging from 0 to 30 kV/cm, specifically due to the transition taking place between the QD bound state and the quasibound state. Only a weak response shoulder at the high-energy end of the spectrum was observed at a higher electric field. It should be

noted that hole levels become denser at the high energy region of the QD potential well. In this Letter, we present a detailed study of the *p*-type valence-band intersublevel transitions. In addition to the QDIP, a DWELL structure is used in order to investigate the effect of QW levels on the *p*-type hole response and its bias dependency. In contrast to *n*-type DWELLs in which different response peaks rise when the applied bias is increased, the spectral range of the response in the *p*-type detector is stationary. Gaussian fittings reveal three individual peaks, corresponding to transitions from QD bound states to the near-barrier QW state. No QD-bound-to-QW-bound transitions can be identified up to the electric field of 54.5 kV/cm. Calculations show that the tunneling probability of holes is less than that of electrons by a factor of more than  $10^3$ – $10^5$ . Because of this, the contribution of QD-bound-to-QW-bound transitions to response is disabled. Although bias-selectable response is enabled in *n*-type DWELLs, this leads to undesired bias-dependent switch from one spectral range to another. Optimum performance of response in a specific wavelength range is therefore unlikely to be achieved by optimizing the bias. Selecting the desired response can be achieved by designing the structures, for examples, using a double-barrier resonant tunneling structure adjacent to the DWELL absorber to filter out unnecessary transitions.<sup>9</sup> In contrast, the *p*-type response naturally displays the single-color characteristic.

The *p*-type hole response spectra of both QDIP and DWELL detectors are analyzed. A schematic of the DWELL structure grown by molecular beam epitaxy is shown in Fig. 1(a). The QDIP used in this study has been reported elsewhere.<sup>1</sup> Figure 1(b) plots the electronic structures of the QDIP and DWELL detector. The DWELL has the same device architecture as the QDIP, except that its absorber consists of 10 periods of InAs QDs, embedded in a 6-nm thick In<sub>0.15</sub>Ga<sub>0.85</sub>As QW. The pyramidal shaped QDs have the height and base dimensions of  $\sim 5$  and  $\sim 20$ – $25$  nm,

<sup>a)</sup>uperera@gsu.edu

respectively. The dot density is about  $5 \times 10^{10} \text{ cm}^{-2}$ . Free holes are introduced into QDs by using a  $\delta$ -doping technique.<sup>1</sup> A sheet density of  $5 \times 10^{11} \text{ cm}^{-2}$   $p$ -type dopants is placed above the QDs, with a 15-nm thick spacer in-between them, which gives about 10 holes per dot.<sup>10</sup> A Perkin-Elmer system 2000 Fourier transform infrared spectrometer is used to measure spectral response of  $400 \times 400 \mu\text{m}^2$  mesas, which have a  $260 \times 260 \mu\text{m}^2$  open area in the center allowing for front-side illumination. A bolometer with known sensitivity is used for background measurements and calibration of the responsivity.

The DWELL detector has two sets of energy levels, corresponding to the QD and QW, respectively. As shown in Fig. 1(b), the  $\text{In}_{0.15}\text{Ga}_{0.85}\text{As}/\text{GaAs}$  QW contains three HH levels (dashed lines), which are obtained using an effective-mass method.<sup>11</sup> It may be noted that the wavefunction of the QW state is influenced by the QD.<sup>12</sup> A simplified model is based on the QW potential embedded with the QD potential (considered as a QW<sup>1</sup>). As can be seen from Fig. 1(b) (dashed-dotted lines), the near-barrier level is not much altered for the computations with and without the QD potential considered. This confirms that photoexcitation from the bound state to the near-barrier state has the dominant contribution to photocurrents. Hence, our simplified computation for the QW is valid for explaining the results. A further study will be needed to fully understand the effect of the QW-QD coupling on the spectral response where bound-to-bound transitions should have distinct contributions to the response. QD levels are also shown (solid lines), calculated using an  $8 \times 8 \mathbf{k} \cdot \mathbf{p}$  model described in Ref. 13. It can be seen that the transitions ending up at the bound states (above the GaAs HH band edge in the valence-band diagram) do not contribute to the response unless photoexcited holes surpass the GaAs barrier. This can be accomplished by a tunneling process, leading to bias-dependent response. For comparison at different biases, response spectra are normalized by multiplying a factor, as shown in Figs. 2(a) and 2(b) for the QDIP and DWELL detector, respectively, where the insets show two primary response peaks at 0.1–0.4 eV (3–12  $\mu\text{m}$ ) and 0.4–0.8 eV (1–3  $\mu\text{m}$ ) due to HH-HH and SO-HH hole transitions, respectively.<sup>1</sup> It can be seen that the spectral response is distinctly different from the  $n$ -type DWELL detectors,<sup>2,3</sup> where the wavelength range of the response varies from the

mid-wavelength infrared to long-wavelength infrared. The emergence of the long-wavelength shoulder (6–12  $\mu\text{m}$ ) at higher negative biases in the QDIP could be associated with the LH-HH transition.<sup>1</sup> For the DWELL detector, no apparent change in the spectral profile of the response is observed.

To identify individual transitions contributing to the spectral response, Gaussian fittings were carried out, using the following formulation:

$$\mathcal{R}(E) = \sum_i \frac{A_i}{\sqrt{2\pi}\sigma_i} \exp\left[-\frac{(E - E_{pi})^2}{2\sigma_i^2}\right], \quad (1)$$

where  $\mathcal{R}$  represents for responsivity.  $E_{pi}$ ,  $A_i$  and  $\sigma_i$  are fitting parameters, denoting the peak energy, amplitude, and the line width, respectively. The full width at half maximum (FWHM) can be calculated from  $\sigma$  by  $2\sqrt{2 \ln 2} \cdot \sigma$ . Representative fittings are shown in Figs. 2(c)–2(f), in which a background signal is deducted from the spectra before the fitting. Figures 3(a)–3(e) summarize the fitting results.

The spectral response of the  $p$ -type QDIP is dominated by a Gaussian peak at low bias, originating from the HH bound-to-HH quasibound transition.<sup>1</sup> An additional high-energy peak occurs at high negative bias and is attributed to be due to the HH bound-to-LH bound transition.<sup>1</sup> For the DWELL detector, three peaks can be resolved. Neither of them can be induced or annihilated by changing the bias. This characteristic indicates the trivial influence of the QD bound-to-QW bound transition on the response, as response based on the bound-to-bound transition should be strongly bias dependent as a consequence of the escape of photoexcited holes through tunneling. Much reduced tunneling probability of holes allows an explanation for this feature. Figure 4 shows calculated tunneling probability based on the Wentzel-Kramers-Brillouin (WKB) approximation, i.e.,

$$T \simeq \exp\left[-2 \int_{z_1}^{z_2} \sqrt{\frac{m^*}{\hbar^2} [V(z) - E]} dz\right], \quad (2)$$

where  $m^*$  is the effective mass,  $V(z)$  is the potential of the barrier,  $E$  is the energy of carriers, and  $z_1$  and  $z_2$  are the turning points. Calculations indicate that the tunneling probability of LH in QDIP and HH in DWELL (through the HH2

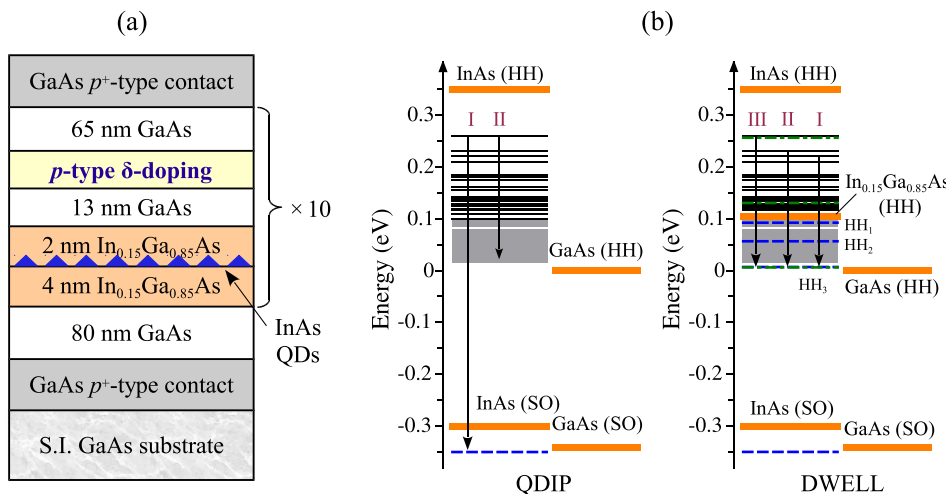


FIG. 1. (a) Schematic of the  $p$ -type DWELL structure. Free holes are introduced into QDs by  $\delta$ -doping above the QD layer. (b) Computed valence band structures of the QDIP and DWELL detector, where solid horizontal lines represent for hole states obtained by using an  $8 \times 8 \mathbf{k} \cdot \mathbf{p}$  model.<sup>13</sup> The thick lines are the band edges. The dashed lines are the calculated HH states of the  $\text{In}_{0.15}\text{Ga}_{0.85}\text{As}/\text{GaAs}$  QW. The dashed-dotted lines are the calculated levels of the DWELL structure where QD is simplified to be a one-dimensional QW.<sup>1</sup> Indicated transitions (I and II for QDIP and I, II, and III for DWELL) agree with the experimental response.

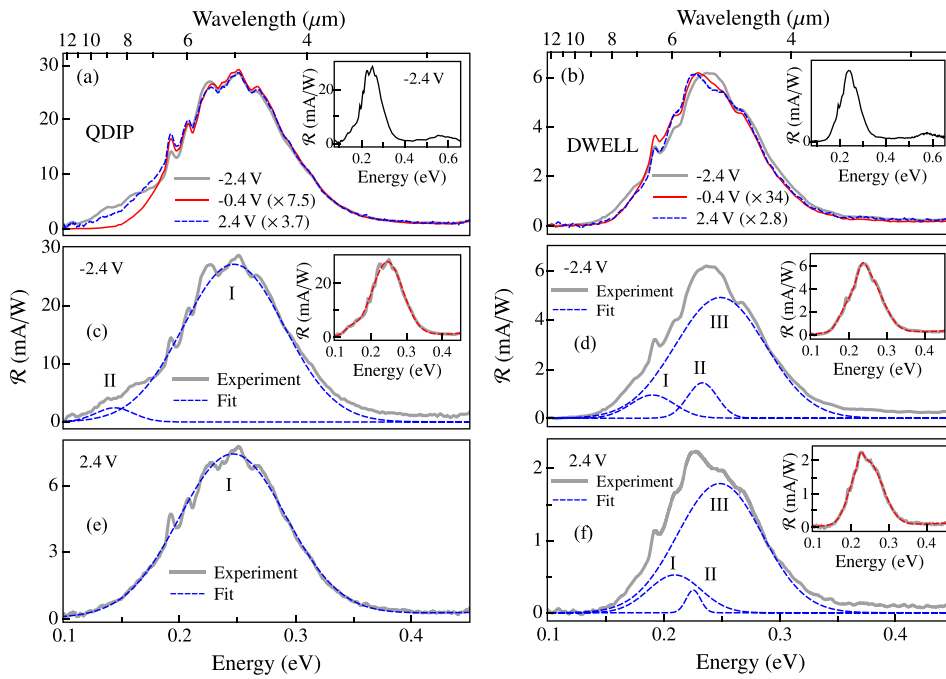


FIG. 2. Normalized spectral response of (a) QDIP and (b) DWELL detector at 78 K, where the insets plot the whole spectral range including a higher-energy peak. (c)–(f) are Gaussian fittings, where each dotted line is the Gaussian components. Insets show the summation of the Gaussian components, in good agreement with the experimental spectra.

level, see Fig. 1(b) are nearly the same. Considering the weak response of the LH-HH transition in QDIP and reduced strength of the 0D QD level-to-1D QW level transition

compared to that of the 0D QD level-to-0D QD level transition, the response due to the 0D QD level-to-1D QW level (HH2) could be even weaker hence not observable

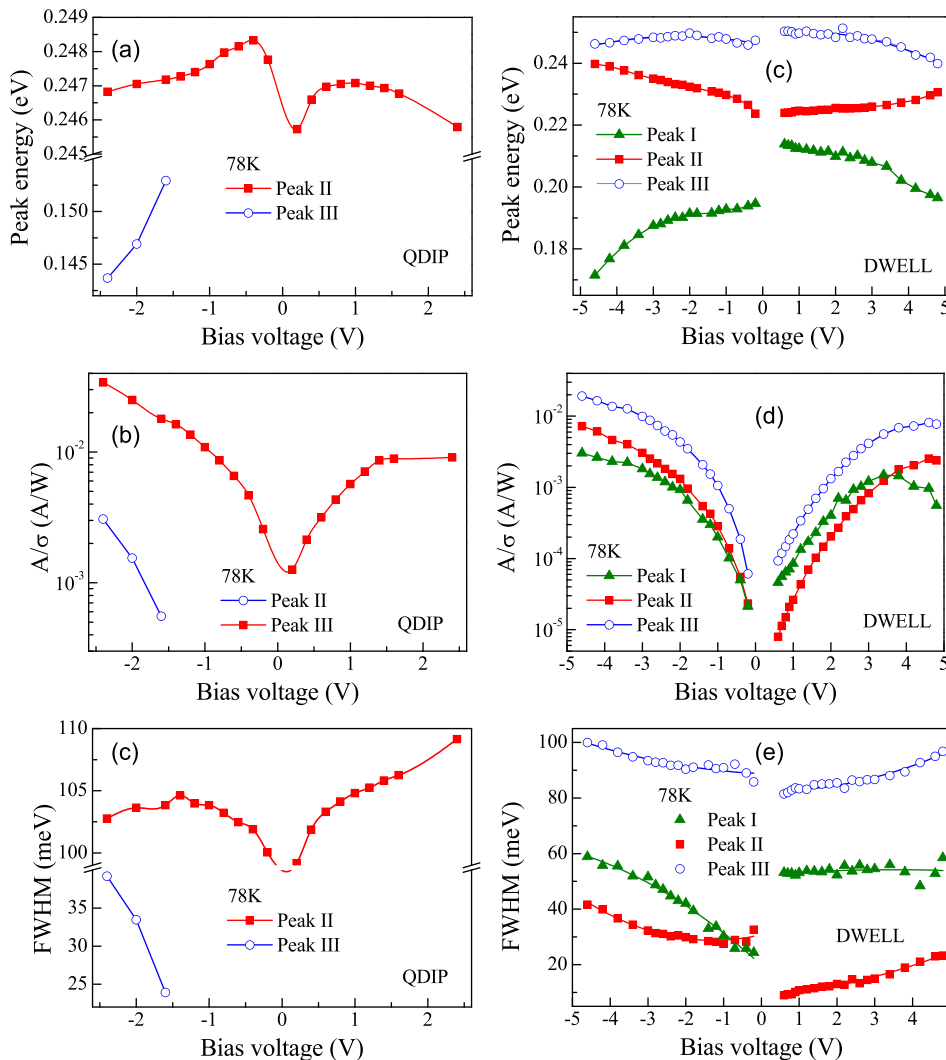


FIG. 3. Fitting results for (a)–(c) QDIP, and (d)–(f) DWELL, where the peak energy,  $A/\sigma$  (see Eq. (1)) and FWHM are plotted as a function of bias.

experimentally. As a comparison, Fig. 4 also shows the calculation for electrons in a dots-in-a-double-well detector reported by Barve *et al.*<sup>9</sup> This *n*-type DWELL structure consists of InAs QDs embedded in a double QW formed by  $\text{Al}_{0.1}\text{Ga}_{0.9}\text{As}/\text{GaAs}/\text{In}_{0.15}\text{Ga}_{0.85}\text{As}/\text{GaAs}/\text{Al}_{0.1}\text{Ga}_{0.9}\text{As}$  layers. The tunneling of electrons starting at the energy level of  $\sim 43$  meV from the  $\text{Al}_{0.1}\text{Ga}_{0.9}\text{As}$  conduction band edge is evaluated. The corresponding response peak is at  $7\ \mu\text{m}$ . More than  $10^3$ – $10^5$  tunneling probability of electrons greater than that of the holes is the reason of bias-dependent response in the *n*-type DWELL detectors, whereas the spectral range of the *p*-type response remains stationary at different biases.

It can be seen from the fitting parameters [Figs. 3(a)–3(e)] that the response behavior is different for forward and reverse biases. Similar observation was obtained in the *n*-type detector.<sup>9</sup> This may be a result of the geometry of the QDs. Further theoretical study will be needed to understand this. By excluding the bound-to-bound transitions, we attribute the three fitted Gaussian peaks for the DWELL detector to be associated with the transitions from the QD ground, first and second excited states to the HH3 QW level, as shown in Fig. 1(b) (I, II, and III). The corresponding transition energies from calculation are 0.215, 0.224, and 0.253 eV, in agreement with the fitting energies, i.e., 0.195–0.214 (I), 0.224 (II), and 0.247–0.250 eV (III) (around 0 V), respectively.

DWELL and QDIP have the similar band profile and hole concentration in the absorber; therefore, their dark currents, which originates from thermionic emission, should be comparable. However, the experimental dark current of DWELL is about 40 times less than that of QDIP, as shown in Fig. 5(a). It can thus be inferred that the distribution of holes in DWELL is sharply different from QDIP. A possible reason is due to the interaction between QD and QW.<sup>2</sup> This may partially explains the lack of the HH bound-to-LH bound transition caused response in the DWELL detector, even at the very high electric field (up to 54.5 kV/cm), as can be seen from the comparison between Figs. 2(a) and 2(b).

By using experimentally measured noise current ( $i_n$ ), the noise gain ( $g$ ) can be calculated through the expression:  $g = i_n^2/4eI_d$ , where  $I_d$  is the dark current [Fig. 5(a)]. Assuming that the photoconductive gain equals the noise gain,<sup>14,15</sup> the value of external QE can be obtained using

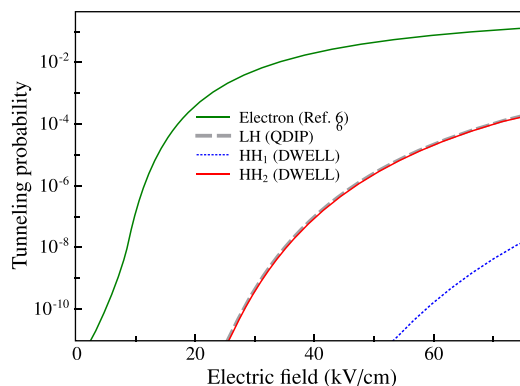


FIG. 4. Comparison of calculated tunneling probability of hole and electron. The calculation of the electron tunneling probability is based on Ref. 9 (dots-in-a-double-well detector). The calculation of LH corresponds to the HH bound-to-LH bound transition, as described in Ref. 1.

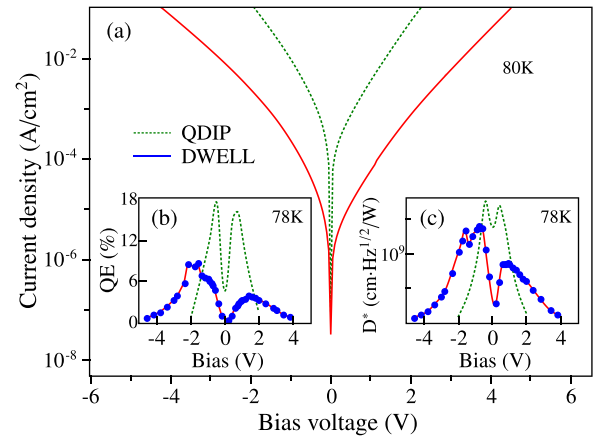


FIG. 5. (a) Dark current density of the *p*-type QDIP and DWELL at 80 K. (b) and (c) (shown as insets) are the QE and specific detectivity (at  $5\ \mu\text{m}$ ), respectively. The QE is obtained by assuming that the photoconductive gain equals the noise gain. The results of DWELL are more asymmetric compared to QDIP probably due to the asymmetry induced by the  $\delta$ -doping.<sup>14,15</sup>

$\text{QE} = \mathcal{R}/g \lambda \times hc/e$ , as shown in Fig. 5(b). As a result of different bias-dependence of  $\mathcal{R}$  and  $g$ , a maximum QE of the DWELL is obtained to be 9% at  $-1.6$  V. The specific detectivity is given by  $D^* = R\sqrt{A \times \Delta f}/i_n$ , where  $A$  is the device area, and  $\Delta f$  is the bandwidth. The detectivity at  $78$  K for the response peak at  $5\ \mu\text{m}$  as a function of bias is shown in Fig. 5(c), with the maximum value at  $1.4 \times 10^9$   $\text{cm}\cdot\text{Hz}^{1/2}/\text{W}$ , which is close to that of the QDIP, as a consequence of the low dark current of the DWELL detector. The improvement of the performance can be achieved by enhancing the absorption. One of the possibilities is to utilize transitions between the bound and bound states, which have the stronger wave-function overlapping than the transitions between the bound and the quasibound/continuum states.

One of the advantages using *p*-type response is its stationary spectral response without showing the bias selectivity. This allows for optimizing the bias for optimum performance at specific wavelengths. The need of tailoring spectral response can be achieved by designing the QW. It is expected that bias dependency can be obtained by moving the HH level closer to the potential barrier in order to increase the tunneling probability. The well-preserved hole response will facilitate the control of the response. Designing multicolor response is also possible by integrating different DWELL structures.

To conclude, we have studied the valence-band intersublevel hole transitions in the *p*-type InAs/GaAs QDIP and DWELL detectors. The DWELL detector displays constant wavelength ranges of response independent of applied biases. Its spectral response results from transitions between QD bound states and near-barrier QW states. This study indicates that the *p*-type QDIP has a well-preserved spectral response, which should benefit the optimization of bias for optimum response and the control of spectral response for the detector development.

This work was supported in part by the U.S. National Science Foundation under Grant No. ECCS-1232184. The Shanghai group acknowledges supports from the National Major Basic Research Projects (2011CB925603), the 863 Program of China (2011AA010205), the Natural Science

Foundation of China (91221201, 61234005, and 11074167). Authors acknowledge the contributions from Professor H. C. Liu, who was involved in the work, until his sudden death in October 2013.

- <sup>1</sup>Y.-F. Lao, S. Wolde, A. G. Unil Perera, Y. H. Zhang, T. M. Wang, H. C. Liu, J. O. Kim, T. Schuler-Sandy, Z.-B. Tian, and S. S. Krishna, *Appl. Phys. Lett.* **103**, 241115 (2013).
- <sup>2</sup>S. Krishna, S. Raghavan, G. von Winckel, A. Stintz, G. Ariyawansa, S. G. Matsik, and A. G. U. Perera, *Appl. Phys. Lett.* **83**, 2745 (2003).
- <sup>3</sup>A. V. Barve and S. Krishna, in *Advances in Infrared Photodetectors. Semiconductors and Semimetal Series*, edited by S. D. Gunapala, D. Rhiger, and C. Jagadish (Elsevier, 2011), Chap. 3, Vol. 84, pp. 153–193.
- <sup>4</sup>A. V. Barve, T. Rotter, Y. Sharma, S. J. Lee, S. K. Noh, and S. Krishna, *Appl. Phys. Lett.* **97**, 061105 (2010).
- <sup>5</sup>S. Deshpande, J. Heo, A. Das, and P. Bhattacharya, *Nat. Commun.* **4**, 1675 (2013).
- <sup>6</sup>V. Ryzhii, *Semicond. Sci. Technol.* **11**, 759 (1996).
- <sup>7</sup>H. C. Liu, F. Szmulowicz, Z. R. Wasilewski, M. Buchanan, and G. J. Brown, *J. Appl. Phys.* **85**, 2972 (1999).
- <sup>8</sup>R. A. Joshi, V. S. Taur, and R. Sharma, *J. Non-Cryst. Solids* **358**, 188 (2012).
- <sup>9</sup>A. Barve, J. Shao, Y. Sharma, T. Vandervelde, K. Sankalp, S. J. Lee, S. K. Noh, and S. Krishna, *IEEE J. Quantum Electron.* **46**, 1105 (2010).
- <sup>10</sup>A. I. Yakimov, A. A. Bloshkin, V. A. Timofeev, A. I. Nikiforov, and A. V. Dvurechenskii, *Appl. Phys. Lett.* **100**, 053507 (2012).
- <sup>11</sup>S. L. Chuang, *Physics of Optoelectronic Devices* (Wiley, New York, 1995).
- <sup>12</sup>L. Höglund, K. F. Karlsson, P. O. Holtz, H. Pettersson, M. E. Pistol, Q. Wang, S. Almqvist, C. Asplund, H. Malm, E. Petrini, and J. Y. Andersson, *Phys. Rev. B* **82**, 035314 (2010).
- <sup>13</sup>H. Jiang and J. Singh, *Phys. Rev. B* **56**, 4696 (1997).
- <sup>14</sup>G. Ariyawansa, A. G. U. Perera, G. Huang, and P. Bhattacharya, *Appl. Phys. Lett.* **94**, 131109 (2009).
- <sup>15</sup>H. Lim, S. Tsao, W. Zhang, and M. Razeghi, *Appl. Phys. Lett.* **90**, 131112 (2007).